ORIGINAL ARTICLE

An Effective Method to Repair Poor Signal of Magnetoencephalography Channel Data

Hanie Arabian [1], Alireza Karimian [1*], Hamid Reza Marateb [1,2], Carolina Migliorelli [3], Miquel Angel Mañanas [2,4], Sergio Romero [2,5], Antonio Russi [6], Rafał Nowak [7]

[1] *Department of Biomedical Engineering, Faculty of Engineering, University of Isfahan, Isfahan, Iran*

[2] *Department of Automatic Control, Biomedical Engineering Research Center, Polytechnic University of Catalonia, BarcelonaTech (UPC), Barcelona, Spain*

[3] *Unit of Digital Health, Eurecat, Centre Tecnològic de Catalunya, 08005 Barcelona, Spain*

[4] *Networking Center in Bioengineering, Biomaterials, and Nanomedicine (CIBER-BBN), Barcelona, Spain*

[5] *CIBER de Bioingeniería, Biomateriales y Nanomedicina (CIBER-BBN), Madrid, Spain*

[6] *Epilepsy Unit, Hospital Quirón Teknon, Barcelona, Spain*

[7] *Magnetoencephalography Unit, Hospital Quirón Teknon, Barcelona, Spain*

*Corresponding Author: Alireza Karimian
Email: karimian@eng.ui.ac.ir

Received: 08 October 2023 / Accepted: 02 December 2023

Abstract

Purpose: Magnetoencephalography is the recording of magnetic fields resulting from the activities of brain neurons and provides the possibility of direct measurement of their activity in a non-invasive manner. Despite its high spatial and temporal resolution, magnetoencephalography has a weak amplitude signal, drastically reducing the signal-to-noise ratio in case of environmental noise. Therefore, signal reconstruction methods can be effective in recovering noisy and lost information.

Materials and Methods: The magnetoencephalography signal of 11 healthy young subjects was recorded in a resting state. Each signal contains the data of 148 channels which were fixed on a helmet. The performance of three different reconstruction methods has been investigated by using the data of adjacent channels from the selected track to interpolate its information. These three methods are the surface reconstruction methods, partial differential equations algorithms, and finite element-based methods. Afterward to evaluate the performance of each method, R-square, root mean square error, and signal-to-noise ratio between the reconstructed signal and the original signal were calculated. The relation between these criteria was checked through proper statistical tests with a significance level of 0.05.

Results: The mean method with the root mean square error of 0.016 ± 0.009 (mean $\pm$ SD) at the minimum time (3.5 microseconds) could reconstruct an epoch. Also, the median method with a similar error but in 5.9 microseconds with a probability of 99.33% could reconstruct an epoch with an R-square greater than 0.7.

Conclusion: The mean and median methods can reconstruct the noisy or lost signal in magnetoencephalography with a suitable percentage of similarity to the reference by using the signal of adjacent channels from the damaged sensor.

Keywords: Data Inpainting; Data Quality Enhancement; Magnetoencephalography; Signal Reconstruction.

Copyright © 2026 Tehran University of Medical Sciences.
This work is licensed under a Creative Commons Attribution-NonCommercial 4.0 International license (https://creativecommons.org/licenses/by-nc/4.0/). Noncommercial uses of the work are permitted, provided the original work is properly cited.
DOI: https://doi.org/10.18502/fbt.v13i2.21940

Frontiers in BIOMEDICAL TECHNOLOGIES

1. Introduction

Investigating brain activity is important because it can provide valuable insights into various aspects of human cognition and behavior. Understanding how the brain functions can help in the development of effective interventions and treatments for neurological and psychological disorders [1]. Brain disorders that can be diagnosed by investigating brain activity include Obsessive-Compulsive Disorder (OCD) [2], stuttering [3], and psychiatric disorders [3]. Identifying activity imbalances in specific brain regions can help diagnose and treat psychiatric disorders.

Electroencephalography (EEG) and Magnetoencephalography (MEG) are relevant to brain activity as they can be used to localize sources of brain electrical activity and evaluate the functional state of the sensorimotor cortex. EEG and MEG measurements provide spatial filtering techniques that enable the localization of closely positioned and possibly highly correlated sources of brain activity, even in low signal-to-noise regimes [4-6]. Additionally, the ~20-Hz brain rhythm, which can be detected by both EEG and MEG, has been used to evaluate sensorimotor cortical functions. Furthermore, EEG and MEG can be used in Non-invasive Transcranial Brain Stimulation (NTBS) techniques to guide the timing and settings of NTBS based on the temporal patterns of ongoing neuronal activity [7].

MEG recordings have been found to produce signals with a higher signal-to-noise ratio with a higher temporal-spatial resolution (1mm-1ms) compared to EEG, making MEG an optimal tool for studying sensorimotor cortical functions [5, 6]. By combining the magnetic field distribution recorded by Superconducting Quantum Interference Device (SQUID) sensors with images of brain anatomy, it is possible to create a reliable functional map of active brain neurons [8, 9].

MEG inverse source reconstruction is a method used to map sensor signals to cortical current sources to investigate brain activity. Several papers discuss different approaches to MEG inverse source reconstruction. Aydin *et al.* present a framework that combines the EEG and MEG information with a volume conductor model of the head to reconstruct the epileptogenic zone in epileptic patients [10]. Piastra *et al.* analyze the effects of brain lesions on MEG source estimates and recommend modeling lesions for accurate reconstruction [11]. Suzuki and Yamashita demonstrate the use of meta-analysis fMRI data to improve current source reconstruction in MEG [12]. O'Neill *et al.* show that incorporating a correlated hippocampal source model improves MEG source estimation [13].

Despite its high spatial resolution, in case of one or some sensor broken, it would be difficult to accurately localize the sources of activity, because of the volume conduction effect, which causes the magnetic fields produced by electrical currents in the brain to spread and overlap [9, 14]. Another limitation is the difficulty in detecting weak electromagnetic sources within the brain. Classical Beamformer, a commonly used MEG source imaging method, may struggle to locate weak sources, especially those that are ipsilateral to the stimulus [15]. Knowing that the number of active neurons is much larger than the number of sensors; therefore, one of the main problems is to determine how the sources are connected, and the spatial arrangement, the orientation, and the periods of neuronal activity are related. A common feature of all neural source reconstruction studies is the complete removal of noisy or low-quality channel data in the signal preprocessing phase [14, 16]. These limitations highlight the need for further advancements in MEG technology and analysis techniques to improve spatial resolution and sensitivity to overcome these challenges in brain imaging.

The studies before did not consider the interpolation and reconstruction of the lost signal of some channels of the MEG signal. Reproducing this information is hence particularly important because noise reduction methods cannot reproduce the signal from these channels. The importance of this research disappears as the amount of information decreases. Reconstructing damaged or lost data can play an important role in better understanding of brain interactions and disorders.

2. Materials and Methods

In this study, a 4D-Neuroimaging device has been used to record the MEG signals. As shown in Figure 1, a helmet with 148 fixed sensors with a 2.5 cm margin from each other has been located above the subjects' heads. Eleven cases aged 30±12 (mean±SD) with no brain disorder at the Barcelona Children's Hospital have participated in the study. The protocol of recording the signal was continuous for a period of 10 minutes with a sampling frequency of 678.17 Hz and without doing any special task.

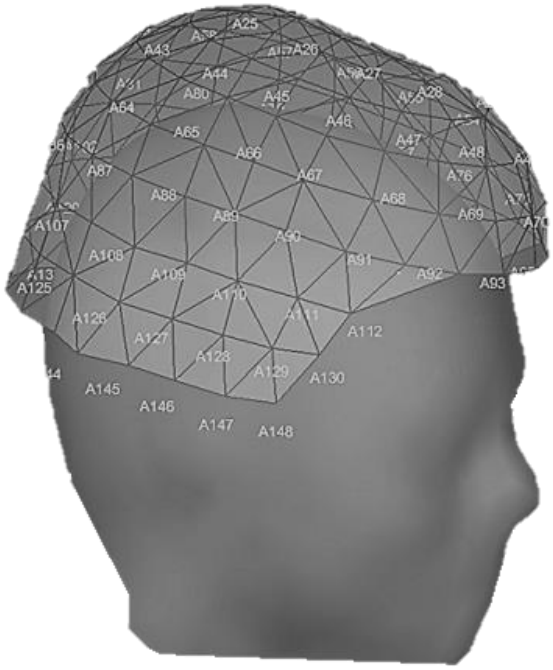


Figure 1. Location of the sensors on the signal recording helmet above the subjects' head (the number after the letter A is the number of each sensor, which ranges from 1 to 148)

2.1. Preprocessing

The suitable frequency range for MEG signals varies depending on the specific study. One study found statistically significant intersubject correlations in MEG signals at frequencies below 10 Hz and a frame rate of 24 Hz [17]. In a study on Autism Spectrum Disorder (ASD), functional connectivity analysis revealed significant hyperconnectivity in the high gamma (50-100 Hz) frequency band [18]. Additionally, a deep learning approach using MEG signals achieved classification accuracy using relative powers of six frequency bands, including delta (1-4 Hz), theta (4-8 Hz), low-alpha (8-10 Hz), high-alpha (10-13 Hz), beta (13-30 Hz), and low-gamma (30-50 Hz) [19]. Overall, the suitable frequency range for MEG signals depends on the specific research question and the neural processes being investigated. Therefore, the combination of a band-pass and band-stop filter was used to strengthen the suitable frequency band of 1 to 90 Hz and weaken the frequency of 50 Hz caused by the noise of city electricity.

2.2. Gold Standard

The signal of each sensor was divided into non-overlapping 500 ms epochs. Afterward, for each epoch, its R-square coefficient was calculated according to Equation 1 with the first and second neighboring sensors. According to the availability of information on the location of each sensor in three directions of X, Y, and Z relative to the reference sensor, to find the neighboring sensors of each sensor, the Euclidean distance of each sensor with all existing sensors was calculated, and based on these distances, the nearest neighbors were identified. If the mean of these coefficients was less than the threshold of 0.5, the signal of the mentioned epoch was removed from the data set as an outlier (Equation 1).

$$R^2 = 1 - \frac{\sum_i (y_i - f_i)^2}{\sum_i (y_i - \bar{y})^2} \quad (1)$$

Where R^2 is the R-square efficient of each epoch with another epoch. y_i and $\bar{y}$ are the time samples of each epoch and its average, respectively. f_i is the time sample of the intended epoch's neighbor.

Epochs with a median R-square coefficient greater than 0.5 were considered as references in this data set. Data normalization was done on the remaining data set.

2.3. Epoch Selection

A set of epochs were randomly selected from the remaining epochs to investigate the performance of reconstruction methods using nearest-neighbor data. This process was done in two stages, once on about 5% and the second on about 15% of all extant epochs.

2.4. Repairing

Four different data interpolating algorithms based on surface reconstruction and Partial Differential Equations (PDE) were utilized. Also, interpolation algorithms based on the Finite Element Method (FEM) were applied to reconstruct the epochs. In each method, the information of several adjacent channels was used in the corresponding time window.

In the two surface reconstruction methods, the 13 nearest neighbors of each sensor were chosen. Next, the mean and/or median of those elected neighbors

were taken using Equations 2 and 3, respectively to reconstruct each randomly selected epoch.

$$\hat{y}_i = \frac{1}{K}\sum_{k=1}^{K} f_{k_i} \quad (2)$$

$$\hat{y}_i = \underset{k=1\ to\ K}{median}(f_{k_i}) \quad (3)$$

Where $\hat{y}_i$ is the ith time sample of the reconstructed epoch corresponding to y_i. K is the number of selected neighbors (here is 13) and f_{k_i} is the ith time sample of kth nearest neighbor.

In using the PDE method, at first, all the sensors had to be mapped from 3 dimensions to 2 dimensions. For this mapping, due to the three-dimensionality of the head shape, one of the spatial dimensions with less variance among the adjacent sensors was eliminated. Therefore, the Euclidean distance of two mapped sensors was calculated just by considering the two remaining dimension locations. Next, the modified Poisson equation according to Equations 4 to 6 used the information of the 8 nearest neighbors of each sensor.

$$g_{k_i} = u_{xx} + u_{yy} \quad (4)$$

$$IC = \frac{1}{K}\sum_{k=1}^{K} g_{k_i} \quad (5)$$

$$\hat{u}_{xx} + \hat{u}_{yy} = IC \quad (6)$$

Where g_{k_i} is the Laplace values of kth nearest neighbor at the ith time sample of an epoch. u_{xx} and u_{yy} are the second-order derivatives of the neighbor signal. IC is the initial condition for each intended sensor. $\hat{u}_{xx}$ and $\hat{u}_{yy}$ are the second-order derivatives of the reconstructed epoch.

In the FEM algorithm, four-node quadrilateral elements are applied using Equations 7 and 8 considering the 4 nearest neighbors.

$$H_k = \frac{(x.x_k + 1)(y.y_k + 1)(z.z_k + 1)}{4} \quad (7)$$

$$\hat{y}_i = \sum_{i=1}^{n} H_k \times V_k \quad (8)$$

Where H_k is a linear matrix of the interpolation function. (x, y, z) and (x_k, y_k, y_k) are the coordinates of the selected sensor and its nearest neighbor coordinates, respectively. k Could be in the range of 1 to 4. V_k is a linear matrix of 4 nearest neighbors' values at ith time sample of the epoch

2.5. Evaluation

R-square coefficient, Root Mean Square Error (RMSE), and Signal-to-Noise Ratio (SNR) between the reference epoch and reconstructed epoch were calculated for each method separately.

Also, to investigate the effect of spatial distribution of corrupted data the Average Nearest Neighbor (ANN) for both stages of randomly selecting epochs was computed. Local Image Contrast (LIC) was measured to examine the effect of the difference between the signal value of each epoch and its neighbors on the performance of each method. Another important factor in evaluating the performance of the reconstruction methods is to inspect the sensitivity of each method to the malfunctioning of the sensors at the borders; therefore, at each stage of choosing epochs for reconstruction, the Percentage of the Outlier Border (POB) was calculated.

The significance of the relation between R-square, RMSE, and SNR criteria with ANN, LIC, and POB was evaluated by a statistical test with a P-value of 0.05.

All stages of data preprocessing and reconstruction algorithms using MATLAB software have been performed by a system with an Intel 7-core processor clocked at 2.6 GHz and 12 GB of RAM.

3. Results

The result of filtering all the channels from the existing data set to strengthen the frequency band 1 to 90 Hz and weaken other frequency bands, especially city electricity noise (range 50 Hz) can be seen in Figure 2. Also, the mean and the standard deviation of SNR in the whole data before preprocessing and after filtering are shown in Figure 3.

Considering that the number of selected epochs for reconstruction was determined in two separate stages

(once for 5% and another time for 15% of all windows), the relations between the percentage of low-quality epochs and the evaluation criteria of the R-square, RMSE, and SNR in each method using the bivariate Pearson correlation statistical test (significance level of P-value < 0.05) are reported in Table 1.

Table 1. The bivariate Pearson correlation statistical test result to investigate the impact of the percentage of low-quality epochs

Method	P-Value		
	R-square	RMSE	SNR
Mean	**0.39**	**0.56**	**0.47**
Median	**0.52**	**0.55**	**0.48**
Modified Poisson	**0.68**	**0.60**	**0.50**
FEM	**0.46**	**0.51**	**0.53**

RMSE = Root Mean Square Error
SNR = Signal-to-Noise Ratio

Due to the lack of impact of the percentage of low-quality epochs on the performance of reconstruction methods to reduce the time and complexity of calculations, the performance of these methods can be evaluated by only 5% of the epochs selected.

The mean and standard deviation of the RMSE of the reconstructed epochs compared to the reference signal and the average required time of a 500-millisecond epoch reconstruction for the introduced methods are reported in Table 2.

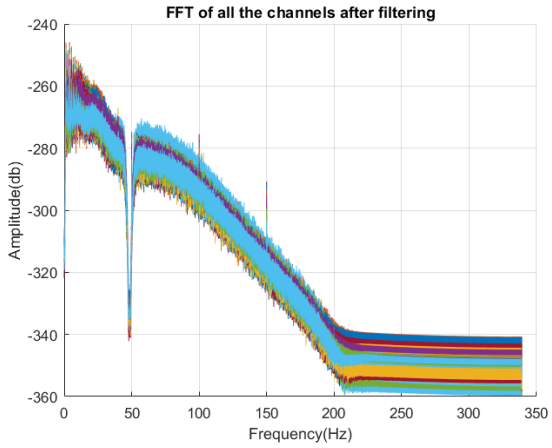


Figure 2. The frequency spectrum of the MEG channels' signal after filtration

The ratio of reconstructed epochs with an R-square greater than 0.70 to all of the reconstructed epochs is reported in Table 3.

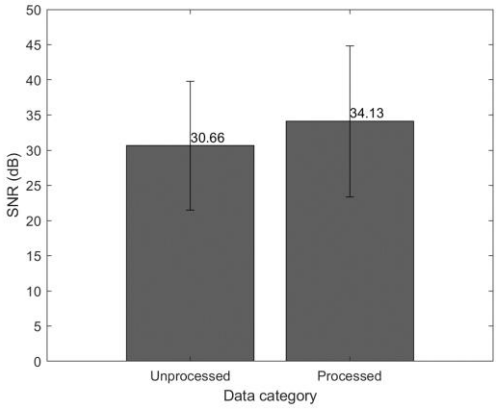


Figure 3. The mean and standard deviation of the SNR of the data before and after pre-processing

The significance level of the relation between the R-square coefficient and SNR with ANN and POB has been examined using the bivariate Pearson correlation statistical test with a significance level of 0.05 in Table 4.

Table 2. The average error and required time for an epoch reconstruction by different reconstruction methods

Method	RMSE (Mean±SD)	Time (μs)
Mean	**0.016±0.009**	**3.5**
Median	**0.016±0.009**	**5.9**
Modified Poisson	**0.021±0.005**	**665.9**
FEM	**0.236±0.813**	**2.9**

Table 3. The percentage of reconstructed epochs with R-square≥0.70 of different reconstruction methods

Method	Percentage (%)
Mean	97.09
Median	99.33
Modified Poisson	52.80
FEM	59.29

The P-value in the bivariate Pearson correlation statistical test to analyze the relation between both R-square and SNR criteria with LIC for all methods was less than 0.05.

Table 4. The P-value of bivariate Pearson correlation statistical test result to investigate the relation between R-square and SNR with ANN and POB

Method	R-square		SNR	
	ANN	POB	ANN	POB
Mean	0.44	0.56	0.61	0.47
Median	0.52	0.53	0.39	0.62
Modified Poisson	0.34	0.49	0.45	0.59
FEM	0.43	0.46	0.54	0.41

ANN = Average Nearest Neighbor
POB = Percentage of the Outlier Border

4. Discussion

MEG is a non-invasive brain imaging method to understand brain functions and disorders better with a high spatial-temporal resolution. In this method, the spatial-temporal distribution of brain magnetic activities is measured without connecting the sensor to the scalp. MEG can discover the brain's active areas during any brain function by using the methods of inverse reconstruction of neural sources [20, 21].

Although the quality of the results of inverse reconstruction is directly related to the increase in the number of sensors, according to the distribution of the magnetic field in the space around each active source, the increase in the number of sensors can lead to an increase in the correlation of sources in the sensors which reduce the accuracy of the known magnetic fields. Therefore, noise or a low signal-to-noise ratio of a channel of magnetoencephalography data leads to errors in the results of inverse reconstruction of the corresponding active nerve source. In recent years, MEG has been used in robotic devices to identify the imagined movement in people with limb paralysis to create a rehabilitation system [20, 21].

As shown in Figure 2, filtering the signal makes it possible to remove the effect of noise caused by the city electricity well, as well as sufficiently weaken the ineffective frequency components. This helps to increase the signal-to-noise ratio so that less noise is involved in signal reconstruction. Also, Figure 3 shows that the mean and standard deviation of the SNR for all channels of all data samples increased from 30.66 ± 9.15 to 34.13 ± 10.67.

After measuring the correlation coefficient and the level of significance of the relation between the criteria of R-square and SNR with the ANN and the POB using the bivariate Pearson correlation statistical test, the P-value for all selected epochs in all methods was more than 0.05. Therefore, there was no significant relationship between these criteria.

Then, to analyze the relation between the R-square and the SNR, with the LIC, using the bivariate Pearson correlation statistical test, the P-value for all the selected epochs in all methods was obtained as less than 0.05. As a result, it is proven that if the signal of the adjacent channels is noisy, the result of signal reconstruction will be affected.

Among the 4 reconstruction methods introduced, the two methods of mean and median with the lowest average and standard deviation of RMSE equal to 0.016±0.009 in the reconstructed epoch showed superior performance compared to the other two methods (on average 0.005 less than the modified Poisson and 0.22 less than FEM). Besides, the highest error was recorded for the FEM method with an average and standard deviation of RMSE equal to 0.236 ± 0.813.

Moreover, the Poisson method with the lowest degree of similarity of the reconstructed signal to the reference signal has taken the longest time (about 665.9 microseconds on average) to reconstruct a 500-millisecond epoch.

The best performance in signal reconstruction is related to the median method from the 13 nearest neighbors of the desired sensor, which was able to reconstruct the signal of 99.33% of test epochs with a high R-square coefficient (greater than 0.7) with an average time of 5.9 microseconds for each one.

After that, the mean method with 13 neighbors could reconstruct the signal of 97.09% (2.24% less than the median method) of the test epochs with an R-square greater than 0.7, with less time (2.4 microseconds) than the median.

5. Conclusion

Generally, in previous MEG studies using visual methods, they identify and remove the undesirable part of the signal (either only in the relevant channel or together with the nearby channels) to minimize the impact of any signal registration error. The performance of inverse neural source reconstruction methods in the presence of damaged channels is difficult or limited. Therefore, interpolating low-quality parts of the signal by considering high-quality signals from nearby channels can improve the performance of the mentioned methods.

Applying the mean or median method from the first and second neighbors of each channel can reconstruct the signal of the mentioned channel with a detection coefficient of more than 0.7 compared to the reference signal with a probability of 99.33% and 97.09%, respectively. The time required to reconstruct the 500-millisecond epoch using these two methods is about 3.5 to 5.9 microseconds on average, which could be momentous if the reconstruction method turned to be online. The importance and innovation of this study is the damaged data reconstruction can be effective in reducing the elimination of data, and subsequently in increasing the results quality of neural sources inverse reconstruction.

In future studies, it is necessary to investigate the effect of the reconstruction of low-quality data from the MEG signal in the inverse neural source reconstruction methods. Also, according to the application of MEG in brain-computer interfaces, it is vital to make the method of identifying and reconstructing the damaged signal online. Due to the automaticity of this study's low-quality signal detection method using similarity criteria such as R-square, the appropriate detection coefficient threshold should also be set automatically. In addition, it is necessary to evaluate the effect of reducing or increasing the number of neighboring sensors participating in the signal reconstruction of each channel on the inverse reconstruction methods.

Acknowledgments

The authors would like to thank the University of Isfahan and the Avicenna Center of Excellence (ACE) for their support. The grant of this research has been registered under the [Grant Number 9912011] in the University of Isfahan.

References

1- Jan-Mathijs Schoffelen and Joachim Gross, "Source connectivity analysis with MEG and EEG." *Human Brain Mapping,* Vol. 30 (No. 6), pp. 1857-65, 2009/06/01 (2009).

2- Vinh Tan *et al.*, "Preliminary Observations of Resting-State Magnetoencephalography in Nonmedicated Children with Obsessive-Compulsive Disorder." *Journal of Child and Adolescent Psychopharmacology,* Vol. 32 (No. 10), pp. 522-32, (2022).

3- Pinar Ozel, Ali Karaca, Ali Olamat, Aydin Akan, Mehmet Akif Ozcoban, and Oguz Tan, "Intrinsic synchronization analysis of brain activity in obsessive–compulsive disorders." *International Journal of Neural Systems,* Vol. 30 (No. 09), p. 2050046, (2020).

4- Mia Illman, Kristina Laaksonen, Mia Liljeström, Veikko Jousmäki, Harri Piitulainen, and Nina Forss, "Comparing MEG and EEG in detecting the~ 20-Hz rhythm modulation to tactile and proprioceptive stimulation." *NeuroImage,* Vol. 215p. 116804, (2020).

5- Gregor Thut *et al.*, "Guiding transcranial brain stimulation by EEG/MEG to interact with ongoing brain activity and associated functions: a position paper." *Clinical Neurophysiology,* Vol. 128 (No. 5), pp. 843-57, (2017).

6- Masashi Sato, Okito Yamashita, Masa-aki Sato, and Yoichi Miyawaki, "Information spreading by a combination of MEG source estimation and multivariate pattern classification." *PloS One,* Vol. 13 (No. 6), p. e0198806, (2018).

7- Pieter Van Mierlo, Yvonne Höller, Niels K Focke, and Serge Vulliemoz, "Network perspectives on epilepsy using EEG/MEG source connectivity." *Frontiers in Neurology,* Vol. 10p. 721, (2019).

8- Mainak Jas, Stephanie R Jones, and Matti S Hämäläinen, "Whole-head OPM-MEG enables noninvasive assessment of functional connectivity." *Trends in Neurosciences,* Vol. 44 (No. 7), pp. 510-12, (2021).

9- Alain de Cheveigné and Dorothée Arzounian, "Robust detrending, rereferencing, outlier detection, and inpainting for multichannel data." *NeuroImage,* Vol. 172pp. 903-12, (2018).

10- Ümit Aydin *et al.*, "Combining EEG and MEG for the Reconstruction of Epileptic Activity Using a Calibrated Realistic Volume Conductor Model." *PloS One,* Vol. 9 (No. 3), p. e93154, (2014).

11- Maria Carla Piastra, Robert Oostenveld, Jan Mathijs Schoffelen, and Vitória Piai, "Estimating the influence of stroke lesions on MEG source reconstruction." *NeuroImage,* Vol. 260p. 119422, (2022).

12- Keita Suzuki and Okito Yamashita, "MEG current source reconstruction using a meta-analysis fMRI prior." *NeuroImage,* Vol. 236p. 118034, (2021).

13- George C O'Neill, Daniel N Barry, Tim M Tierney, Stephanie Mellor, Eleanor A Maguire, and Gareth R Barnes, "Testing covariance models for MEG source reconstruction of hippocampal activity." *Scientific Reports,* Vol. 11 (No. 1), p. 17615, (2021).

14- Makoto Fukushima, Okito Yamashita, Thomas R Knösche, and Masa-aki Sato, "MEG source reconstruction based on identification of directed source interactions on whole-brain anatomical networks." *NeuroImage,* Vol. 105pp. 408-27, (2015).

15- Amit Jaiswal *et al.*, "Comparison of beamformer implementations for MEG source localization." *NeuroImage,* Vol. 216p. 116797, (2020).

16- John G Samuelsson, Noam Peled, Fahimeh Mamashli, Jyrki Ahveninen, and Matti S Hämäläinen, "Spatial fidelity of MEG/EEG source estimates: A general evaluation approach." *NeuroImage,* Vol. 224p. 117430, (2021).

17- Kaisu Lankinen, Jukka Saari, Riitta Hari, and Miika Koskinen, "Intersubject consistency of cortical MEG signals during movie viewing." *NeuroImage,* Vol. 92pp. 217-24, (2014).

18- Kasturi Barik, Katsumi Watanabe, Joydeep Bhattacharya, and Goutam Saha, "Functional connectivity based machine learning approach for autism detection in young children using MEG signals." *Journal of Neural Engineering,* Vol. 20 (No. 2), p. 026012, (2023).

19- Jo Aoe *et al.*, "Automatic diagnosis of neurological diseases using MEG signals with a deep neural network." *Scientific Reports,* Vol. 9 (No. 1), p. 5057, (2019).

20- Alexander E Hramov, Vladimir A Maksimenko, and Alexander N Pisarchik, "Physical principles of brain–computer interfaces and their applications for rehabilitation, robotics and control of human brain states." *Physics Reports,* Vol. 918pp. 1-133, (2021).

21- Luke Tait, Ayşegül Özkan, Maciej J Szul, and Jiaxiang Zhang, "A systematic evaluation of source reconstruction of resting MEG of the human brain with a new high-resolution atlas: Performance, precision, and parcellation." *Human Brain Mapping,* Vol. 42 (No. 14), pp. 4685-707, (2021).